

Article

Preparation and Characterisation of Cellulose Nanocrystal/Alginate/Polyethylene Glycol Diacrylate (CNC/Alg/PEGDA) Hydrogel Using Double Network Crosslinking Technique for Bioprinting Application

Anusha Wei Asohan ¹, Rokiah Hashim ², Ku Marsilla Ku Ishak ³ , Zuratul Ain Abdul Hamid ³ , Nurshafiqah Jasme ¹ and Yazmin Bustami ^{1,*} 

¹ School of Biological Sciences, Universiti Sains Malaysia, Gelugor 11800, Malaysia; anushawei96@gmail.com (A.W.A.); nurshafiqahjasme@gmail.com (N.J.)

² Division of Bioresource, Paper and Coatings Technology, School of Industrial Technology, Universiti Sains Malaysia, Gelugor 11800, Malaysia; hrokiah@gmail.com

³ School of Materials and Mineral Resources Engineering, USM Engineering Campus, Universiti Sains Malaysia, Nibong Tebal 14300, Malaysia; ku_marsilla@usm.my (K.M.K.I.); srzuratulain@usm.my (Z.A.A.H.)

* Correspondence: ybustami@usm.my

Abstract: In this study, we aimed to prepare and characterise hydrogel formulations using cellulose nanocrystals (CNCs), alginate (Alg), and polyethylene glycol diacrylate (PEGDA). The CNC/Alg/PEGDA formulations were formed using a double network crosslinking approach. Firstly, CNC was extracted from oil palm trunk, and the size and morphology of the CNCs were characterised using TEM analysis. Secondly, different formulations were prepared using CNCs, Alg, and PEGDA. The mixtures were crosslinked with Ca²⁺ ions and manually extruded using a syringe before being subjected to UV irradiation at 365 nm. The shear-thinning properties of the formulations were tested prior to any crosslinking, while the determination of storage and loss modulus was conducted post extrusion after the Ca²⁺ ion crosslink using a rheometer. For the analysis of swelling behaviour, the constructs treated with UV were immersed in PBS solution (pH 7.4) for 48 h. The morphology of the UV crosslinked construct was analysed using SEM imaging. The extracted CNC exhibited rod-like structures with an average diameter and length of around 7 ± 2.4 and 113 ± 20.7 nm, respectively. Almost all CNC/Alg/PEGDA formulations (pre-gel formulation) displayed shear-thinning behaviour with the power-law index $\eta < 1$, and the behaviour was more prominent in the 1% [w/v] Alg formulations. The CNC/Alg/PEGDA with 2.5% and 4% [w/v] Alg displayed a storage modulus dominance over loss modulus ($G' > G''$) which suggests good shape fidelity. After the hydrogel constructs were subjected to UV treatment at 365 nm, only the F8 construct [4% CNC: 4% Alg: 40% PEGDA] demonstrated tough and flexible characteristics that possibly mimic the native articular cartilage property due to a similar water content percentage (79.5%). In addition, the small swelling ratio of 4.877 might contribute to a minimal change of the 3D construct's geometry. The hydrogel revealed a rough and wavy surface, and the pore size ranged from 3 to 20 μm . Overall, the presence of CNCs in the double network hydrogel demonstrated importance and showed positive effects towards the fabrication of a potentially ideal 3D bioprinted scaffold.

Keywords: cellulose nanocrystals; alginate; polyethylene glycol diacrylate; biomaterials; bioprinting



Citation: Asohan, A.W.; Hashim, R.; Ku Ishak, K.M.; Abdul Hamid, Z.A.; Jasme, N.; Bustami, Y. Preparation and Characterisation of Cellulose Nanocrystal/Alginate/Polyethylene Glycol Diacrylate (CNC/Alg/PEGDA) Hydrogel Using Double Network Crosslinking Technique for Bioprinting Application. *Appl. Sci.* **2022**, *12*, 771. <https://doi.org/10.3390/app12020771>

Academic Editor: Jinah Jang

Received: 30 November 2021

Accepted: 3 January 2022

Published: 13 January 2022

Publisher's Note: MDPI stays neutral with regard to jurisdictional claims in published maps and institutional affiliations.



Copyright: © 2022 by the authors. Licensee MDPI, Basel, Switzerland. This article is an open access article distributed under the terms and conditions of the Creative Commons Attribution (CC BY) license (<https://creativecommons.org/licenses/by/4.0/>).

1. Introduction

The articular cartilage is a specialised connective tissue that provides a low-friction, lubricated, and load-bearing surface for efficient joint movement. However, its compositional and structural nature is easily disrupted with overuse, trauma, or degenerative diseases [1]. Any injury to the articular cartilage can lead to progressive impairment of the joint structure, which is one of the major causes of joint pain and chronic disability that lasts

for years [2,3]. Unlike bones, which have the natural ability to heal over time, the articular cartilage, unfortunately, has a limited capacity for self-repair due to the absence of blood vessels, making treatment efforts a challenge [1,3]. Current treatments used in clinical practice include symptomatic and restoration procedures [2,4]. Symptomatic treatments are generally prescribed painkillers and non-steroidal anti-inflammatory drugs (NSAIDs) that offer pain relief while restoration treatments utilise surgical approaches which involve reconstructing the damaged articular cartilage and total joint replacement. However, these treatments require prolonged rehabilitation and complications can arise, such as donor shortage and immunologic response associated with these methods [2,4].

Research on tissue-engineered articular cartilage has led to many promising tissue constructs *in vitro*, however, phenotypically stable mature chondrocyte cells and functionally equivalent engineered articular cartilage constructs remain elusive and are often hampered by a limited control over the scaffold structure and mechanical and biological complexities [2,4]. The emerging three-dimensional (3D) bioprinting technology permits a superior solution to address cartilage repair limitations. In general, 3D bioprinting is a subset of 3D printing technology that dispenses bioink by fabricating 3D scaffolds in a layer-by-layer manner. This technique allows the 3D scaffolds to mimic the native architecture of the cartilage which allows better cell-to-cell communication [5]. There are different kinds of bioprinting setup including extrusion-based, particle fusion-based, light-induced, and inkjet-based [5,6]. The bioink consists of a selection of suitable biomaterials and living cells that can promote tissue regeneration [6]. The selection of an ideal bioink is important in order to maintain the articular cartilage tissue's organised architecture. An ideal bioink should satisfy certain requirements, such as good mechanical properties, printability, and bio-compatibility [7]. The challenge lies in formulating a bioink that meets all these requirements. For bioinks used in cartilage bioprinting, the bioink needs to be tough and load bearing while also having elastic tendencies [8].

There are two main groups of biomaterials: namely, natural polymers and synthetic polymers which are usually used in bioink formulations. Natural polymers such as alginate have been used extensively in regenerative medicine due to its intrinsic properties that are akin to human tissues [9]. Alginate also has a unique sol/gel transition that allows the conversion between semisolid and solid state, which is highly favourable in bioprinting applications [10]. However, despite its promising features, alginate possesses several disadvantages that limit its use in 3D bioprinting. Some of the major concerns include being mechanically weak, having poor stability, and lacking the capability to adhere to mammalian cells [11]. Alginate can form a hydrogel via ionic crosslinking with cations like Ca^{2+} to improve its mechanical strength and stability. However, this physical crosslinking is unstable and not long lasting as the crosslinked alginate hydrogels can be reversed and eventually cause the alginate hydrogel to disintegrate due to the displacement of the divalent cations (Ca^{2+}) by the monovalent cations (Na^+) which are normally present in the culture medium [12]. This drawback can be overcome by the addition of other biomaterials as a reinforcing agent and the introduction of a secondary crosslinking mechanism via chemical crosslinking which will give rise to a more stable hydrogel [13].

The mechanical properties of alginate hydrogel can be improved by the addition of cellulose nanocrystals (CNCs) as a reinforcement material [14]. In general, CNCs have many unique properties that are highly desirable in biomedical applications. Some of which include its high aspect ratio, availability, abundance in nature, and sustainability [15]. In 3D bioprinting applications, CNCs are often used as rheological modifiers and reinforcing agents for hydrogels due to their high crystallinity [14]. Several studies report that the addition of nanocellulose greatly improved the printability of alginate-based hydrogels [16–18]. During the extrusion process, it was also reported that the printed structures not only retained their shape with minimal spreading but also had improved geometries [19,20]. While the addition of CNCs as a reinforcing agent improves the strength and printability of hydrogels, a stronger support system is required to produce a tough and flexible hydrogel that can mimic the native articular cartilage [21].

The introduction of a second network can help to achieve this requirement. This technique is also known as the double network (DN) system [21,22]. A double network hydrogel improves the mechanical properties due to the presence of interpenetrating networks, which is a desirable property for cartilage bioprinting applications [13]. Double network hydrogels are currently studied with the intention to overcome the limitation of weak and brittle hydrogels. A study done by Hong et al. confirmed this hypothesis by successfully forming highly stretchable and tough double network hydrogels for 3D bioprinting [21]. Synthetic polymers like polyethylene glycol diacrylate (PEGDA) can be combined with natural polymers to form a double network hydrogel through photopolymerization. Several literatures have reported good cell viability while using low concentrations (ranging from 0.01% to 0.1%) of Irgacure 2959 (I-2959) and short UV exposure times (ranging from 1 to 10 min) in their study [3,23–25]. Cui et al. also reported the promising cell viability of human articular chondrocytes in their photopolymerised bioink with a cell viability of $63.2 \pm 9.0\%$ in the post printing polymerisation which increased to $89.2 \pm 3.6\%$ when simultaneous polymerisation was applied [3]. Irgacure 2959 has been the photoinitiator of choice as it is the least toxic among other photoinitiators (Irgacure 184 and Irgacure 651) and causes minimal cell death when tested over a broad range of mammalian cell types [24]. PEGDA is widely recognised as a successful scaffolding material in tissue engineering due to its biocompatibility and low immunogenicity [26]. PEGDA-based hydrogels are also resistant to protein adhesion, making them ideal scaffolds that can promote cell growth and differentiation towards the formation of tissues [27].

Hence, this study attempted to produce bioink using different concentration of CNC, Alg, and PEGDA and to utilise the double network crosslinking technique that may satisfy the requirement for cartilage bioprinting.

2. Materials and Methods

2.1. Materials

Sodium alginate, calcium sulphate, and polyethylene glycol diacrylate (PEGDA) with a molecular weight of (Mn) 700 g/mol, and phosphate-buffered saline were purchased from Sigma Aldrich (St. Louis, MO, USA). Photoinitiator 2-Hydroxy-4'-(2-hydroxyethoxy)-2-methylpropiophenone (Irgacure 2959) was purchased from PENCHEM (Simpang Ampat, Penang, Malaysia). Glacial acetic acid, ethanol, toluene, potassium hydroxide, and sulfuric acid were purchased from QRëC (Rawang, Selangor, Malaysia). Sodium chlorite was purchased from Acros Organics (Fair Lawn, NJ, USA). The oil palm trunk fibres were provided by the School of Industrial Technology, USM, Penang Malaysia. All chemicals were used as received.

2.2. Isolation and Extraction of Cellulose Nanocrystal

The extraction of the cellulose nanocrystal was carried out using the acid hydrolysis procedure as described in references [28,29] with slight modifications. Firstly, raw oil palm trunk fibres were ground into fine powder using the Riken grinder with a 1.5 mm filter screen. The fibre extractives were dewaxed for 4 h through the Soxhlet extraction method using ethanol/toluene [2:1 (v/v)] and were dried overnight in the oven at 40 °C. Secondly, about 20 g of the dried fibre sample was bleached in a sodium chlorite (NaClO₂) solution under an acidic condition (10% acetic acid solution) at 70 °C under agitation of 70 rpm in a water bath incubator shaker for 1 h, and this step was repeated 4 times. The bleached fibres were washed vigorously with dH₂O until the fibres change to a white colour. The hemicelluloses region of the fibres was eliminated by soaking the fibres in 6 wt% potassium hydroxide (KOH) for one day at 4 °C. Then, the fibres were repeatedly washed with dH₂O to neutralize the pH of the samples and were further processed using the acid-hydrolysis technique. About 210 mL of sulfuric acid solution (64%; H₂SO₄) was added to the sample and was agitated at 45 °C for 1 h. Subsequently, about 400 mL of cold water was added to the hydrolysed cellulose fibres, followed by washing and rinsing using dH₂O at least 15 times. Any residual sulfuric acid was further eliminated by subjecting it

to a dialysis process for at least 3 days in order to neutralise the pH. The samples were then homogenised and sonicated before being subjected to a freeze-dried process. The dried CNC was stored at RT until further use.

Characterisation Using TEM Analysis

The structure and size of the CNCs were observed using transmission electron microscopy (TEM) (EFTEM Libra 120, Carl Zeiss, Germany). This analysis was conducted at the Electron Microscopy Unit, School of Biological Sciences, Universiti Sains Malaysia. The measurement of the CNCs was done using ImageJ software (Version 1.53) and the average value of the data was reported.

2.3. Preparation and Formulation of CNC/Alg/PEGDA Scaffolds

About nine formulations were prepared by mixing different concentrations of CNC [2% & 4%; (*w/v*)], Alg [1%, 2.5% & 4% (*w/v*)], and PEGDA; MW:700 g/mol [10% & 40% (*v/v*)] as listed in Table 1. Firstly, an equal volume of CNC and PEGDA solutions were mixed well using a magnetic stirrer. The Alg solution was then added into the CNC/PEGDA mixture and mixed well using a magnetic stirrer to form a homogenous CNC/Alg/PEGDA pre-gel mixture (Figure 1A). Secondly, 0.05% (*w/v*) photoinitiator I-2959 and 1% (*w/v*) CaSO₄ were added to the mixture solution to form a soft gel (Figure 1B). The schematic illustration of the preparation, crosslinking, and extrusion process is shown in Figure 2. The CNC/Alg/PEGDA mixture was loaded into a 5 mL syringe and allowed to stand for about 10 min to allow the crosslinking process. Subsequently, the CNC/Alg/PEGDA mixture was extruded manually into a glass mould (Figure 2B). Finally, after the extrusion was completed, the construct was irradiated using UV irradiation at 365 nm with a portable UV lamp for about 10 min before being rinsed with dH₂O to remove any excess crosslinkers (Figure 2C).

Table 1. CNC/Alg/PEGDA formulations.

Formulation	CNC% (<i>w/v</i>)	Alg% (<i>w/v</i>)	PEGDA% (<i>v/v</i>)
F1	0	1	10
F2	4	1	10
F3	0	1	40
F4	4	1	40
F5	0	4	10
F6	4	4	10
F7	0	4	40
F8	4	4	40
F9	2	2.5	25

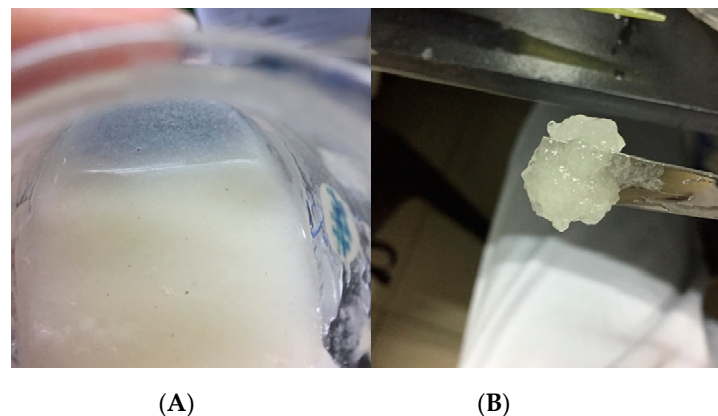


Figure 1. CNC/Alg/PEGDA pre-gel formulation in liquid form (A), and CNC/Alg/PEGDA gelled formulation after the addition of CaSO₄ (B).

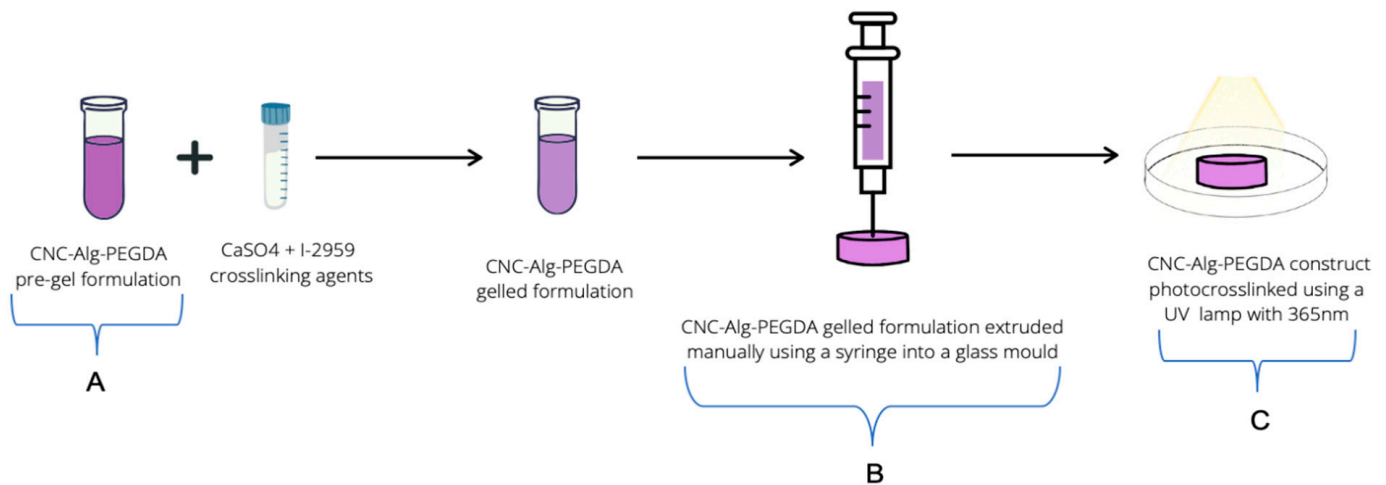


Figure 2. Schematic illustration of the manual extrusion process of CNC/Alg/PEGDA formulations. The important process includes (A) pre-gel formulation preparation, (B) extrusion of hydrogel into a glass mould, and (C) construct treated with UV irradiation at 365 nm post extrusion.

2.4. Rheological Analysis of CNC/Alg/PEGDA Formulations

The rheology analysis was carried out at the School of Materials and Mineral Resources Engineering, USM. The analysis was carried out using Anton Paar MCR 301 with cone-plate (CP25-2, diameter of 25 mm, angle of 2° and gap width of 104 μm). All measurements were conducted in triplicate at RT. Steady-state shear rate viscosity of the selected pre-gel formulations (without the presence of any crosslinkers) was conducted over a range of shear rate of 10 to 1000 s⁻¹. The CNC/Alg/PEGDA formulations were crosslinked with CaSO₄ prior to oscillation frequency measurements. A minute amount of the gelled sample was extruded onto the plate of the rheometer. Oscillation amplitude sweeps were first performed to determine the linear viscoelastic region (LVR) from 0.1 to 100% at a fixed frequency of 1 Hz (Figures S1–S4). From the LVR, a strain of 0.1% was chosen as it was found to be within the LVR for all the gelled formulations. The oscillation frequency measurements were then performed at a frequency range of 1 to 100 Hz using the 0.1% strain.

2.5. Compression Tests of Mechanical Properties of CNC/Alg/PEGDA Construct

The mechanical properties of the constructs post extrusion with UV treatment were manually tested. This technique was adopted from the method reported in reference [30] with some modifications. About 1 mL of the gelled CNC/Alg/PEGDA formulations was extruded into the glass mould (Figure 3B) and irradiated using a portable UV lamp of 365 nm for 10 min (Figure 3C). The post UV crosslinked constructs were removed using a small spatula. The constructs were then compressed by applying some force using a universal glass bottle filled with water and released shortly after. The condition of the constructs before and after compression was observed.

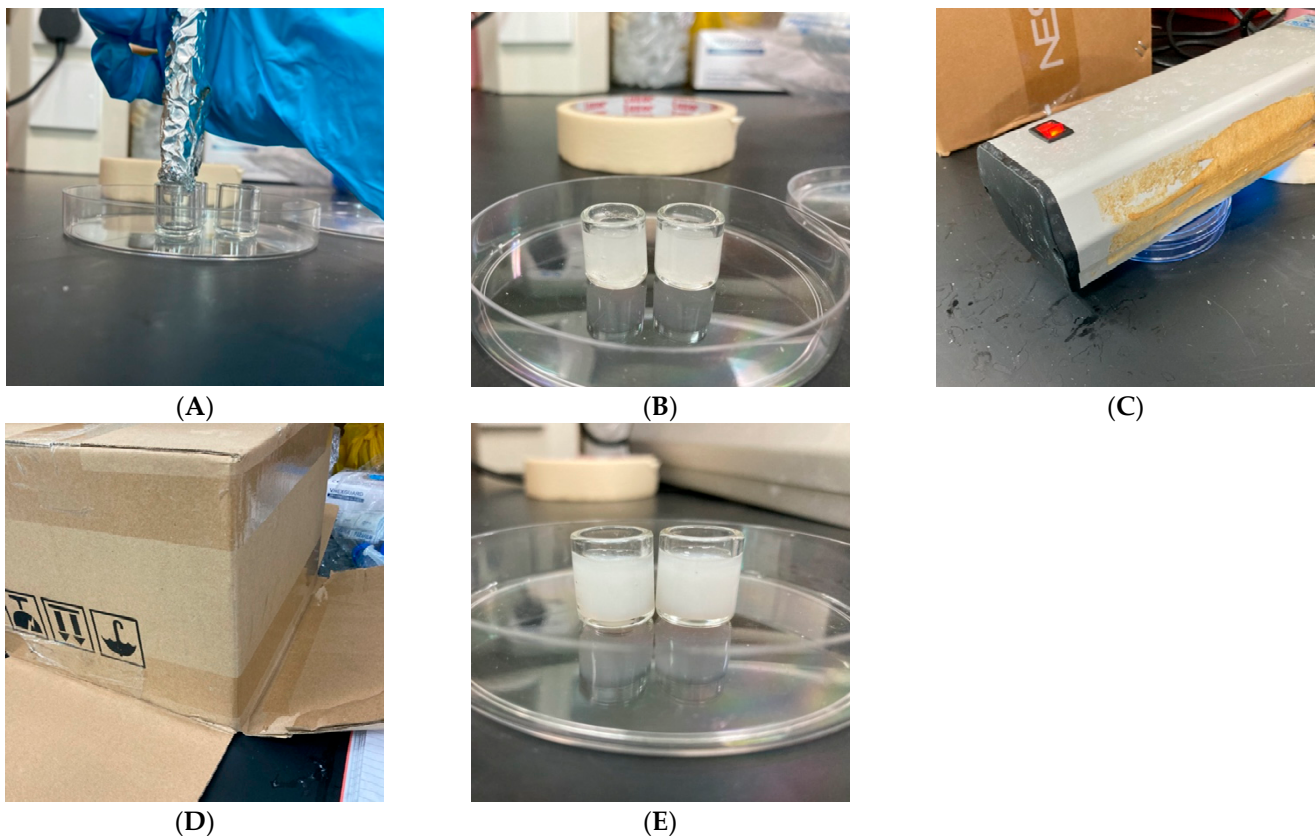


Figure 3. CNC/Alg/PEGDA gelled formulation extruded into glass mould (A), gelled CNC/Alg/PEGDA formulation in glass mould (B), UV irradiation using portable UV lamp with 365 nm (C), UV irradiation process carried out covered with a box (D), and CNC/Alg/PEGDA constructs post UV irradiation (E).

2.6. Swelling Studies of CNC/Alg/PEGDA Constructs

CNC/Alg/PEGDA hydrogel constructs post UV irradiation were first air-dried at RT for 72 h to obtain the dry weight. Then, the dried constructs were immersed in PBS solution, pH of 7.4 for 48 h, and the swollen constructs were weighed. PBS solution was used as it has physiological conditions that are isotonic and non-toxic to cells and tissues. Any excess water on the sample surface was removed using filter paper. The water content (M) and equilibrium mass swelling ratio (Q) of the constructs were determined by the equations shown in (1) and (2), respectively:

$$\text{Water content}(M) = \frac{W_s - W_d}{W_s} \times 100\% \quad (1)$$

$$\text{Mass swelling ratio}(Q) = \frac{W_s}{W_d} \quad (2)$$

where W_s and W_d represent the weight of the constructs after equilibrium swelling in the PBS solution and the dry weight of the constructs, respectively (2). The swelling studies were conducted in triplicates.

2.7. Morphology of CNC/Alg/PEGDA 3D Constructs

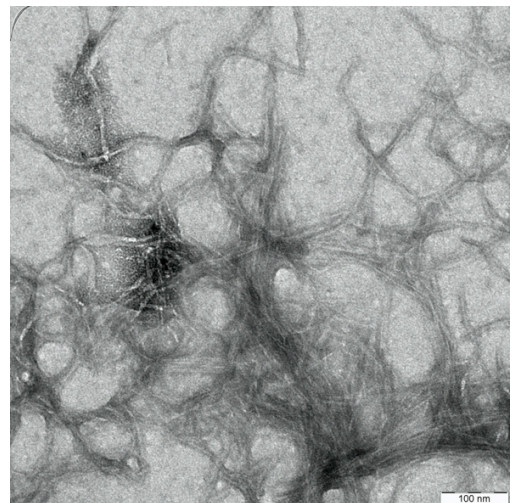
The 3D internal structure of CNC/Alg/PEGDA (F8: [4% CNC: 4% Alg: 40% PEGDA]) was examined using a field emission scanning electron microscope (FESEM, ZeissSupra 55 VP). Upon crosslinking with CaSO_4 , the hydrogel sample was extruded into a glass mould and irradiated with UV at 365 nm for 10 min. The UV crosslinked construct was then removed from the glass mould and sliced into small pieces and subsequently frozen

at $-80\text{ }^{\circ}\text{C}$ and freeze-dried. The freeze-dried samples were then placed in a sputter coater, and the sample surface was coated with gold for FESEM observation. The morphology of the construct porosity was observed, and the pore size was measured using ImageJ Software.

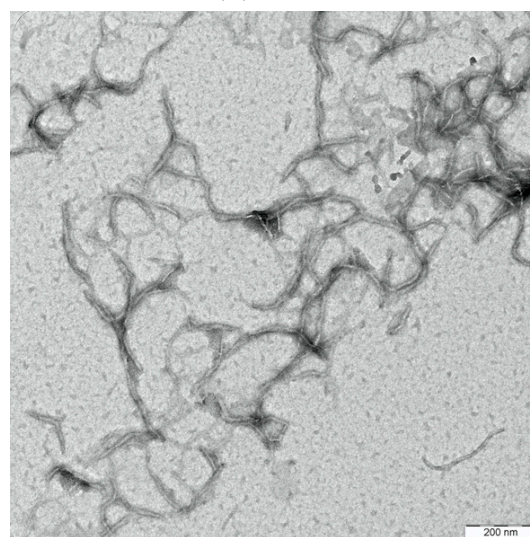
3. Results and Discussion

3.1. Yield and Properties of Cellulose Nanocrystals

In this study, the yield of cellulose nanocrystals (CNC) extracted from oil palm trunk (OPT) is approximately 34%. The yield was within the expected efficiency range of 21–44% when a high sulfuric acid concentration (64–65%) was used [29,31,32]. Despite the lower yield, acid hydrolysis is a commonly used method for CNC extraction as CNCs with a higher stability and pure crystalline region can be obtained [32,33]. Figure 4 presents the TEM image of the CNC after the extraction process. The CNC exhibited typical rod-like structures with an average diameter and length of around 7 ± 2.4 and 113 ± 20.7 nm, respectively. Generally, CNCs have a broad distribution of geometric dimensions, and the size of nanocrystals are varied, with a diameter of around 2–20 nm and a length of around 100–600 nm [33,34] depending on the preparation methods and the cellulose source.



(A)



(B)

Figure 4. TEM image of CNC extracted from oil palm trunk (OPT) after acid hydrolysis treatment with magnification of (A) $40,000\times$ and (B) $20,000\times$.

3.2. Rheological Analysis of CNC/Alg/PEGDA Formulations

3.2.1. Shear-Thinning Properties of Pre-Gel Formulations

As seen in Table 2, the power-law index (η) and consistency index (K) shows the prediction of the extrusion behaviour of the pre-gel formulations. When the power-law index is $\eta < 1$, the fluid displays shear-thinning properties whereas when $\eta = 1$, the fluid displays Newtonian behaviour. The results revealed that pre-gel formulation without CNCs displayed near Newtonian behaviour, showing very limited to no shear-thinning behaviour over the range of shear rates. However, it was observed that the addition of CNCs in the Alg/PEGDA pre-gel formulations reduced the power-law index, η , indicating shear-thinning property. In Figures 5 and 6, the pre-gel formulations with the presence of CNC [F2, F4, F6, F8, and F9] mostly showed shear-thinning behaviours where the viscosity decreased with increasing shear rate. Shear-thinning property is required in extrusion bioprinting as it improves the printability of the bioink by reducing flow resistance through the disturbance of the crosslinked systems [13]. Additionally, the liquid-like state of the bioink generated during the extrusion process at a high shear rate could shield the cells from any shear stress [13,35]. Interestingly, at low Alg concentrations [1% (w/v)], the shear-thinning behaviour of the CNC/Alg/PEGDA pre-gel formulations is more pronounced than at high Alg concentrations [2.5 and 4% (w/v)]. This observation suggests that the increase in the Alg concentration might hinder the effect of CNCs within the hydrogel network. Hence, this finding highlights the importance of CNC in the formulation, as it could improve the shear-thinning property. This result is also in agreement with other studies; Refs. [18,20,36] reported that the addition of nanocellulose in the bioink increased shear-thinning behaviour.

Table 2. Power-law index (η) and consistency index (K) for the different CNC/Alg/PEGDA pre-gel formulations.

Formulation	CNC (% w/v)	Alginate (% w/v)	PEGDA (% v/v)	Power-Law Index (η)	Consistency Index, K (Pa)
1	0	1	10	0.916	0.0094
2	4	1	10	0.645	0.2135
3	0	1	40	0.912	0.0157
4	4	1	40	0.054	13.15
5	0	4	10	0.913	0.0183
6	4	4	10	0.861	0.0863
7	0	4	40	0.696	1.4541
8	4	4	40	0.747	0.4719
9	2	2.5	25	0.744	0.0805

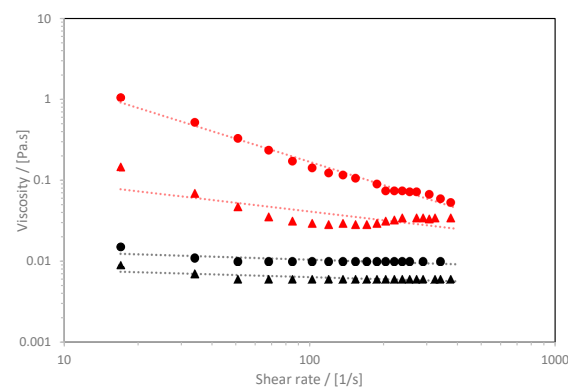


Figure 5. Flow curves of four different CNC/Alg/PEGDA pre-gel formulations indicating shear-thinning properties: (●) F4: [4% CNC: 1% Alg: 40% PEGDA]; (▲) F2: [4% CNC: 1% Alg: 10% PEGDA]; (●) F3: [1% Alg: 40% PEGDA]; and (▲) F1: [1% Alg: 10% PEGDA]. Data points represent actual data, and lines are power-law model fits.

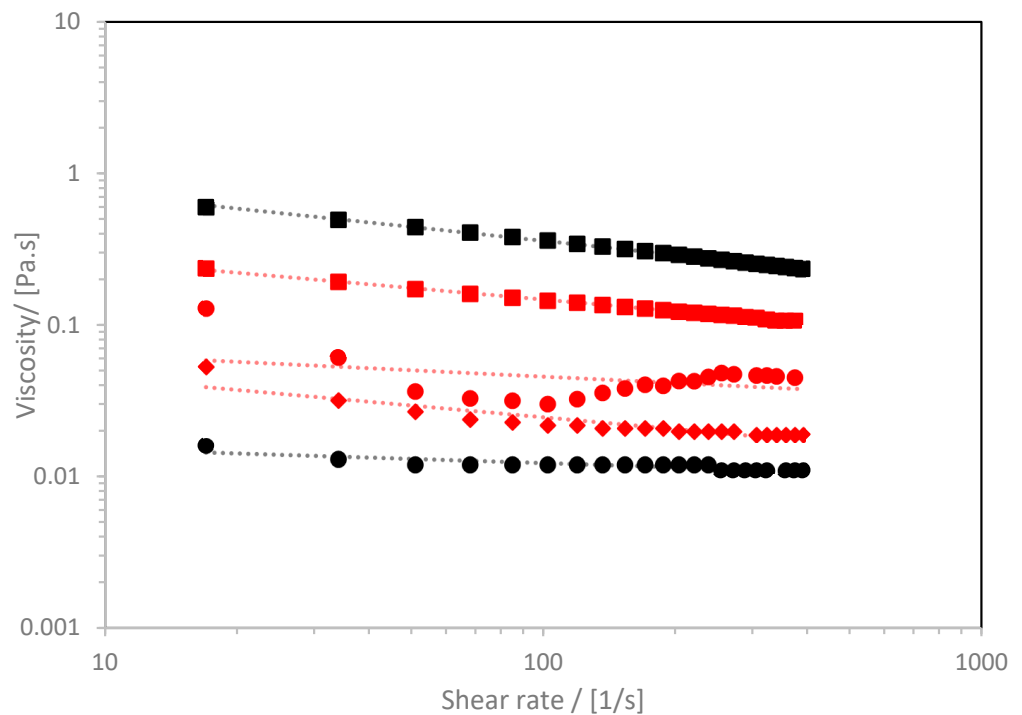


Figure 6. Flow curves of five different CNC/Alg/PEGDA pre-gel formulations indicating shear-thinning properties: (■) F7: [4% Alg: 40% PEGDA]; (■) F8: [4% CNC: 4% Alg: 40% PEGDA]; (●) F6: [4% CNC: 4% Alg: 10% PEGDA]; (◆) F9: [2% CNC: 2.5% Alg: 25% PEGDA]; and (●) F5: [4% Alg: 10% PEGDA]. Data points represent actual data, and lines are power-law model fits.

On the other hand, the flow curve for F7 [4% Alg: 40% PEGDA] displayed shear-thinning property even without the addition of CNCs. This may be due to the unique interaction and entanglement between Alg and PEGDA at these particular concentrations which makes them easier to be aligned under high shear rates [22].

3.2.2. Determination of Storage and Loss Moduli of CNC/Alg/PEGDA Gelled Formulations

The determination of the storage and the loss modulus of the Ca^{2+} gelled formulations was conducted post extrusion and revealed that only F6, F7, F8, and F9 could be detected by the rheometer (2.5 and 4% [w/v] Alg). While the remaining formulations with 1% [w/v] Alg concentration (F1 to F5) were unable to be detected, possibly due to their weak structures. Figure 7 presents the storage and loss modulus values of the different gelled formulations. The dominance of the storage modulus (G') over the loss modulus (G'') value ($G' > G''$) suggests that the tested formulation displayed a continuous firm solid-gel network. Furthermore, no crossover could be observed between the storage and loss modulus at any point of the frequency range. This consistency suggests that the gelled formulations are able to retain their shapes with good shape fidelity post extrusion [37,38]. It is important to note that bioinks with good shape fidelity will contribute to high accuracy and resolution of a printed scaffold. This finding also corroborated that the addition of CNC has a positive effect on the shape fidelity of the gelled formulations, probably due to the increased interactions between the hydrogel networks [16,18].

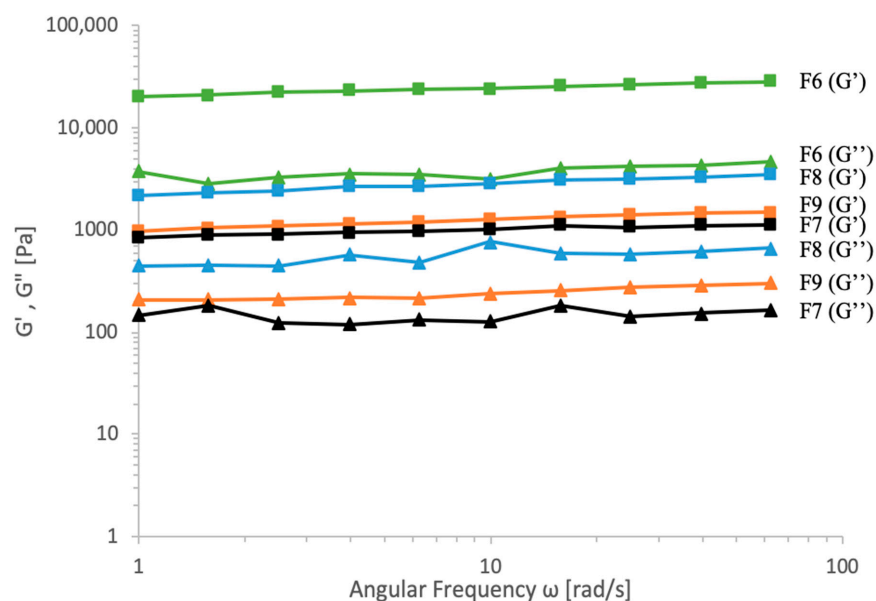


Figure 7. Determination of storage modulus, G' (square symbol), and loss modulus, G'' (triangle symbol), of four gelled formulations; F6: [4% CNC: 4% Alg: 10% PEGDA]; F7: [4% Alg: 40% PEGDA]; F8: [4% CNC: 4% Alg: 40% PEGDA]; and F9: [2% CNC:2.5% Alg:25% PEGDA].

3.3. CNC/Alg/PEGDA Scaffold

3.3.1. Physical Characteristics and Elastic-like Structure of CNC/Alg/PEGDA Scaffold

Upon manual extrusion and double crosslinking treatment using ionic (Ca^{2+}) and UV irradiation at 365 nm, the physical characteristics of the CNC/Alg/PEGDA formulations were observed. Only one formulation, F8 [4% CNC: 4% Alg: 40% PEGDA], satisfied the requirement for cartilage bioprinting. As observed in Figure 8, the construct with the presence of CNCs (F8) appeared as spongy and elastic-like. In fact, this formulation was able to recover to its original shape after it had been compressed (Figure 9). In contrast, the formulation without CNCs, F7 [4% Alg: 40% PEGDA], appeared to be rigid and brittle. Moreover, when subjected to the compression test, it easily broke. Hence, it was corroborated that the presence of CNCs resulted in a firm and flexible construct. This may be attributed to the distribution of the CNCs within the hydrogel network that creates a structured space between the crosslinked polymers, preventing the formation of a dense and tight network [39]. Furthermore, a well-distributed network within the hydrogel increases the tendency of the construct to be less brittle and become more elastic [40]. This result is consistent with other studies that reported that nanocellulose greatly affects the compression modulus of a hydrogel [41]. This characteristic is favourable for soft tissue engineering since it mimics the elastic properties of the native soft tissue.

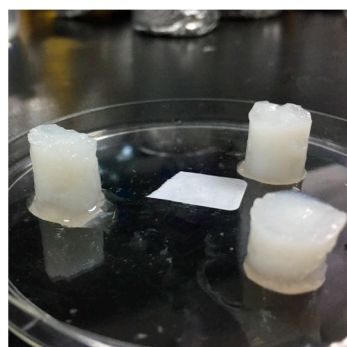


Figure 8. The physical appearance of construct F8 [4% CNC: 4% Alg: 40% PEGDA].

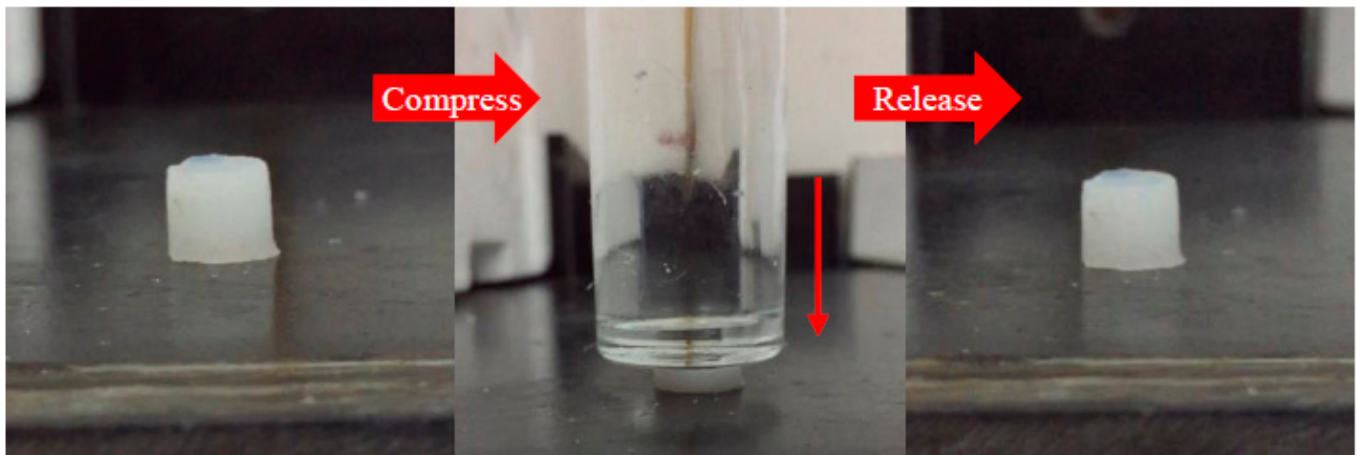


Figure 9. Observation of the elastic-like structure of the construct F8 [4% CNC: 4% Alg: 40% PEGDA] by manual compression test.

3.3.2. Swelling Properties of CNC/Alg/PEGDA Constructs

When immersed in PBS solution (pH 7.4) for 48 h, all the constructs remained stable and did not degrade until they reached the swelling equilibrium. This suggests that the double network (DN) approach contributes to good structural stability as the structure was retained even after immersion in the buffer medium. This observation provides information on the construct's behaviour in a buffer medium. It is an important requirement for scaffolds to maintain their shapes in culture medium where the cells will grow and take over the scaffold [42].

As presented in Table 3, when the concentration of Alg and PEGDA in the formulations increased, the equilibrium water content and swelling ratio decreased; noting that there is an increase in crosslinking within the hydrogel network [43]. This phenomenon might be due to the reduction of empty spaces within the hydrogel network which could lower the water absorbance capability. This finding also suggests a strong interaction between Alg and PEGDA since no obvious differences were observed when CNC was added. Since there is a limited amount of information on the crosslinking and interactions between CNC, Alg, and PEGDA, further research on this interaction needs to be conducted.

Table 3. Water Content and Swelling Ratio of CNC/Alg/PEGDA 3D construct.

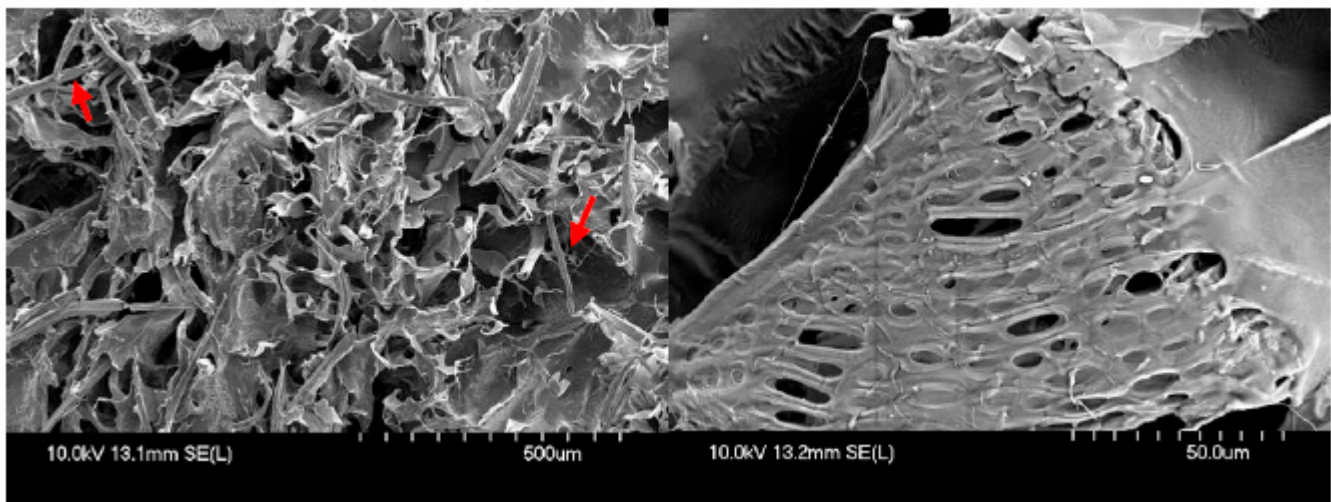
Formulation	CNC (% w/v)	Alg (% w/v)	PEGDA (% v/v)	Equilibrium Water Content (%)	Equilibrium Swelling Ratio
1	0	1	10	95.8	25.37
2	4	1	10	91.9	12.30
3	0	1	40	85.1	7.43
4	4	1	40	86.9	7.62
5	0	4	10	82.3	5.67
6	4	4	10	84.0	6.25
7	0	4	40	80.2	5.32
8	4	4	40	79.5	4.88
9	2	2.5	25	86.1	7.23

In general, high water content is common in hydrogel due to its biomimicry property [44]. However, hydrogel with a water content greater than 90% is very weak and has a limited practical application in tissue engineering [45]. Due to this reason, a suitable formulation is crucial to balance between sufficient water content and mechanical strength. Therefore, only the F8 construct [4% CNC: 4% Alg: 40% PEGDA] showed both preferred characteristics. F8 has a water content of 79.5%, which is similar to the water content percentage in native articular cartilage: 78–80% [3,46]. Hence, F8 can possibly mimic the

properties of native articular cartilage and can also provide load support at optimum hydration levels [47]. In addition, it showed a small swelling ratio, 4.877, which is preferred in bioprinting application since the swelling ratio affects the geometry of the construct [48]. A minimal change in the geometry of the printed 3D construct is expected from a small swelling ratio.

3.3.3. Morphology of CNC/Alg/PEGDA 3D Constructs

The SEM micrographs show the morphology of the F8 [4% CNC: 4% Alg: 40% PEGDA] construct. The CNCs indicated by the arrows are attached to the hydrogel surface, resulting in an entangled network (Figure 10A). This unique entanglement seems to have a positive effect on the toughness and flexibility of the construct. The SEM micrographs also show that the hydrogel has a rough and wavy surface which indicates a tough network [49]. A rough surface is also more favourable for cell growth and attachment as it has a closer resemblance to the native tissue. According to a study done by Hatano et al., osteoblast cells effectively attached and increased proliferation and differentiation on rough surfaces as compared to smooth surfaces [50]. The pores within the CNC/Alg/PEGDA construct ranged from 3 to 20 μm . The presence of pores within a scaffold is important to encourage cell proliferation and to promote the transport of gases and nutrients to the cells [51]. Upon further magnification (801 \times), the SEM micrographs reveal a close-up view of the pores which have irregular oblong shapes as opposed to the conventional circular shape (Figure 10B). This observation indicates that there was shrinkage of the hydrogel leading to the distortion of the pore structures. According to previous studies, drying the hydrogel samples using liquid nitrogen before freeze-drying, also known as the cryo-fixing approach, for sample drying preparation is more favourable for maintaining the native structure of the hydrogel sample and, thus, should be taken into consideration for future SEM analysis [52,53].



(A)

(B)

Figure 10. Scanning electron micrographs of freeze-dried F8 [4% CNC: 4% Alg: 40% PEGDA] construct at magnification of (A) 100 \times and (B) 801 \times . CNC fibres indicated with arrows.

4. Conclusions

In this preliminary study, we successfully produced different formulations using CNC, Alg, and PEGDA for bioprinting applications. CNCs extracted from oil palm trunk exhibited a typical rod-like structure with an average diameter and length of around 7 ± 2.4 and 113 ± 20.7 nm, respectively. Almost all the pre-gel formulations of CNC/Alg/PEGDA displayed shear-thinning behaviour, most prominently in 1% [w/v] Alg formulations with power-law index $\eta < 1$. For post extrusion gelled formulations, CNC/Alg/PEGDA with

2.5% and 4% [w/v] Alg showed storage modulus dominance over loss modulus ($G' > G''$) suggesting a good shape fidelity. After the constructs were subjected to UV treatment at 365 nm, only the F8 construct [4% CNC: 4% Alg: 40% PEGDA] demonstrated the tough and flexible characteristics that are favourable for cartilage bioprinting. It can possibly mimic the properties of the native articular cartilage due to a similar water content percentage (79.5%) and the small swelling ratio (4.877) that might contribute to a minimal change of the 3D construct geometry. From the SEM analysis, the UV crosslinked constructs revealed a rough and wavy surface, and the pore size ranged from 3 to 20 μm . Overall, the presence of CNCs in the double network hydrogel is seemingly important and shows positive effects towards the fabrication of a potential bioink. However, further analysis on the CNC/Alg/PEGDA formulation, such as biocompatibility and cytotoxicity, printability using a 3D bioprinter, and the degradation properties, should be evaluated to make a conclusive stand on its suitability as a bioink for cartilage bioprinting applications.

Supplementary Materials: The following are available online at <https://www.mdpi.com/article/10.3390/app12020771/s1>, Figure S1: Oscillation amplitude sweep (0.1–100%) of F6: [4% CNC: 4% Alg: 10% PEGDA] hydrogel with a fixed frequency of 1 Hz. Figure S2: Oscillation amplitude sweep (0.1–100%) of F7: [4% Alg: 40% PEGDA] hydrogel with a fixed frequency of 1 Hz. Figure S3: Oscillation amplitude sweep (0.1–100%) of F8: [4% CNC: 4% Alg: 40% PEGDA] hydrogel with a fixed frequency of 1 Hz. Figure S4: Oscillation amplitude sweep (0.1–100%) of F9: [2% CNC: 2.5% Alg: 25% PEGDA] hydrogel with a fixed frequency of 1 Hz

Author Contributions: Conceptualization, Y.B.; formal analysis, A.W.A.; funding acquisition, R.H., K.M.K.I., Z.A.A.H. and Y.B.; investigation, A.W.A.; methodology, A.W.A. and N.J.; project administration, N.J.; resources, R.H. and K.M.K.I.; supervision, Y.B.; validation, Z.A.A.H.; writing—original draft, A.W.A.; writing—review & editing, Y.B. All authors have read and agreed to the published version of the manuscript.

Funding: This work is supported financially by the Ministry of Higher Education Malaysia with Fundamental Research Grant Scheme with Project Code: FRGS/1/2018/STG05/USM/02/6.

Institutional Review Board Statement: Not applicable.

Informed Consent Statement: Not applicable.

Data Availability Statement: All relevant data are within the paper.

Acknowledgments: The authors would like to thank the School of Industrial Technology, USM for providing the oil palm trunk fibres and the use of the lab for the isolation and extraction of the cellulose nanocrystals (CNCs) used in this study.

Conflicts of Interest: The authors declare no conflict of interest.

References

1. Sophia Fox, A.J.; Bedi, A.; Rodeo, S.A. The basic science of articular cartilage: Structure, composition, and function. *Sports Health* **2009**, *1*, 461–468. [[CrossRef](#)]
2. Medvedeva, E.V.; Grebenik, E.A.; Gornostaeva, S.N.; Telpuhov, V.I.; Lychagin, A.V.; Timashev, P.S.; Chagin, A.S. Repair of Damaged Articular Cartilage: Current Approaches and Future Directions. *Int. J. Mol. Sci.* **2018**, *19*, 2366. [[CrossRef](#)]
3. Cui, X.; Breitenkamp, K.; Finn, M.G.; Lotz, M.; D’Lima, D.D. Direct human cartilage repair using three-dimensional bioprinting technology. *Tissue Eng.-Part A* **2012**, *18*, 1304–1312. [[CrossRef](#)]
4. Żylińska, B.; Silmanowicz, P.; Sobczyńska-Rak, A.; Jarosz, Ł.; Szponder, T. Treatment of Articular Cartilage Defects: Focus on Tissue Engineering. *Vivo* **2018**, *32*, 1289–1300. [[CrossRef](#)]
5. Agarwal, S.; Saha, S.; Balla, V.K.; Pal, A.; Barui, A.; Bodhak, S. Current Developments in 3D Bioprinting for Tissue and Organ Regeneration—A Review. *Front. Mech. Eng.* **2020**, *6*, 90. [[CrossRef](#)]
6. Morgan, F.L.C.; Moroni, L.; Baker, M.B. Dynamic Bioinks to Advance Bioprinting. *Adv. Health Mater.* **2020**, *9*, 1901798. [[CrossRef](#)]
7. Gu, Z.; Fu, J.; Lin, H.; He, Y. Development of 3D bioprinting: From printing methods to biomedical applications. *Asian J. Pharm. Sci.* **2019**, *15*, 529–557. [[CrossRef](#)]
8. Xu, T.; Binder, K.W.; Albanna, M.Z.; Dice, D.; Zhao, W.; Yoo, J.J.; Atala, A. Hybrid printing of mechanically and biologically improved constructs for cartilage tissue engineering applications. *Biofabrication* **2013**, *5*, 015001. [[CrossRef](#)]
9. Axpe, E.; Oyen, M.L. Applications of Alginate-Based Bioinks in 3D Bioprinting. *Int. J. Mol. Sci.* **2016**, *17*, 1976. [[CrossRef](#)]

10. Hospodiuk, M.; Dey, M.; Sosnoski, D.; Ozbolat, I.T. The bioink: A comprehensive review on bioprintable materials. *Biotechnol. Adv.* **2017**, *35*, 217–239. [[CrossRef](#)]
11. Li, H.; Tan, C.; Li, L. Review of 3D printable hydrogels and constructs. *Mater. Des.* **2018**, *159*, 20–38. [[CrossRef](#)]
12. Hoffman, A.S. Hydrogels for biomedical applications. *Adv. Drug Deliv. Rev.* **2012**, *64*, 18–23. [[CrossRef](#)]
13. Chimene, D.; Kaunas, R.; Gaharwar, A.K. Hydrogel Bioink Reinforcement for Additive Manufacturing: A Focused Review of Emerging Strategies. *Adv. Mater.* **2019**, *32*, e1902026. [[CrossRef](#)] [[PubMed](#)]
14. Gauss, C.; Pickering, K.L.; Muthe, L.P. The use of cellulose in bio-derived formulations for 3D/4D printing: A review. *Compos. Part C Open Access* **2021**, *4*, 100113. [[CrossRef](#)]
15. Shankaran, D.R. Cellulose Nanocrystals for Health Care Applications. In *Applications of Nanomaterials*; Woodhead Publishing: Cambridge, UK, 2018; pp. 415–459. [[CrossRef](#)]
16. Han, C.; Wang, X.; Ni, Z.; Ni, Y.; Huan, W.; Lv, Y.; Bai, S. Effects of nanocellulose on Alginate/Gelatin Bioinks for Extrusion-based 3D Printing. *BioResources* **2020**, *15*, 7357–7373. [[CrossRef](#)]
17. Müller, M.; Öztürk, E.; Arlov, Ø.; Gatenholm, P.; Zenobi-Wong, M. Alginate Sulfate–Nanocellulose Bioinks for Cartilage Bioprinting Applications. *Ann. Biomed. Eng.* **2017**, *45*, 210–223. [[CrossRef](#)]
18. Markstedt, K.; Mantas, A.; Tournier, I.; Ávila, H.M.; Hägg, D.; Gatenholm, P. 3D Bioprinting Human Chondrocytes with Nanocellulose–Alginate Bioink for Cartilage Tissue Engineering Applications. *Biomacromolecules* **2015**, *16*, 1489–1496. [[CrossRef](#)]
19. Nguyen, D.; Hägg, D.A.; Forsman, A.; Ekholm, J.; Nimkingratana, P.; Brantsing, C.; Kalogeropoulos, T.; Zaunz, S.; Concaro, S.; Brittberg, M.; et al. Cartilage Tissue Engineering by the 3D Bioprinting of iPS Cells in a Nanocellulose/Alginate Bioink. *Sci. Rep.* **2017**, *7*, 658. [[CrossRef](#)]
20. Wu, Y.; Lin, Z.Y.; Wenger, A.C.; Tam, K.C.; Tang, X. 3D bioprinting of liver-mimetic construct with alginate/cellulose nanocrystal hybrid bioink. *Bioprinting* **2018**, *9*, 1–6. [[CrossRef](#)]
21. Hong, S.; Sycks, D.; Chan, H.F.; Lin, S.; Lopez, G.P.; Guilak, F.; Leong, K.W.; Zhao, X. 3D Printing of Highly Stretchable and Tough Hydrogels into Complex, Cellularized Structures. *Adv. Mater.* **2015**, *27*, 4035–4040. [[CrossRef](#)]
22. Zhou, W.; Zhang, H.; Liu, Y.; Zou, X.; Shi, J.; Zhao, Y.; Ye, Y.; Yu, Y.; Guo, J. Sodium alginate-polyethylene glycol diacrylate based double network fiber: Rheological properties of fiber forming solution with semi-interpenetrating network structure. *Int. J. Biol. Macromol.* **2019**, *142*, 535–544. [[CrossRef](#)]
23. Nguyen, T.; Watkins, K.E.; Kishore, V. Photochemically crosslinked cell-laden methacrylated collagen hydrogels with high cell viability and functionality. *J. Biomed. Mater. Res. Part A* **2019**, *107*, 1541–1550. [[CrossRef](#)]
24. Williams, C.G.; Malik, A.N.; Kim, T.K.; Manson, P.N.; Elisseff, J.H. Variable cytocompatibility of six cell lines with photoinitiators used for polymerizing hydrogels and cell encapsulation. *Biomaterials* **2005**, *26*, 1211–1218. [[CrossRef](#)] [[PubMed](#)]
25. Fedorovich, N.E.; Oudshoorn, M.H.; van Geemen, D.; Hennink, W.E.; Alblas, J.; Dhert, W.J. The effect of photopolymerization on stem cells embedded in hydrogels. *Biomaterials* **2009**, *30*, 344–353. [[CrossRef](#)]
26. Hamid, Z.A.; Lim, K. Evaluation of UV-crosslinked Poly(ethylene glycol) Diacrylate/Poly(dimethylsiloxane) Dimethacrylate Hydrogel: Properties for Tissue Engineering Application. *Procedia Chem.* **2016**, *19*, 410–418. [[CrossRef](#)]
27. Liu, S.Q.; Tay, R.; Khan, M.; Ee, P.L.R.; Hedrick, J.L.; Yang, Y.Y. Synthetic hydrogels for controlled stem cell differentiation. *Soft Matter* **2009**, *6*, 67–81. [[CrossRef](#)]
28. Fahma, F.; Iwamoto, S.; Hori, N.; Iwata, T.; Takemura, A. Isolation, preparation, and characterization of nanofibers from oil palm empty-fruit-bunch (OPEFB). *Cellulose* **2010**, *17*, 977–985. [[CrossRef](#)]
29. Lamaming, J.; Hashim, R.; Sulaiman, O.; Leh, C.P.; Sugimoto, T.; Nordin, N.A. Cellulose nanocrystals isolated from oil palm trunk. *Carbohydr. Polym.* **2015**, *127*, 202–208. [[CrossRef](#)]
30. Lu, Y.; He, W.; Cao, T.; Guo, H.; Zhang, Y.; Li, Q.; Shao, Z.; Cui, Y.; Zhang, X. Elastic, Conductive, Polymeric Hydrogels and Sponges. *Sci. Rep.* **2014**, *4*, srep05792. [[CrossRef](#)]
31. Hamad, W.Y.; Hu, T.Q. Structure-process-yield interrelations in nanocrystalline cellulose extraction. *Can. J. Chem. Eng.* **2010**, *88*, 392–402. [[CrossRef](#)]
32. Wang, Q.Q.; Zhu, J.Y.; Reiner, R.S.; Verrill, S.P.; Baxa, U.; McNeil, S.E. Approaching zero cellulose loss in cellulose nanocrystal (CNC) production: Recovery and characterization of cellulosic solid residues (CSR) and CNC. *Cellulose* **2012**, *19*, 2033–2047. [[CrossRef](#)]
33. Phanthong, P.; Reubroycharoen, P.; Hao, X.; Xu, G.; Abudula, A.; Guan, G. Nanocellulose: Extraction and application. *Carbon Resour. Convers.* **2018**, *1*, 32–43. [[CrossRef](#)]
34. Islam, M.N.; Rahman, F. Production and modification of nanofibrillated cellulose composites and potential applications. In *Green Composites for Automotive Applications*; Woodhead Publishing: Cambridge, UK, 2019; pp. 115–141.
35. Paxton, N.; Smolan, W.; Böck, T.; Melchels, F.; Groll, J.; Jungst, T. Proposal to assess printability of bioinks for extrusion-based bioprinting and evaluation of rheological properties governing bioprintability. *Biofabrication* **2017**, *9*, 044107. [[CrossRef](#)]
36. Hou, K.; Li, Y.; Liu, Y.; Zhang, R.; Hsiao, B.S.; Zhu, M. Continuous fabrication of cellulose nanocrystal/poly(ethylene glycol) diacrylate hydrogel fiber from nanocomposite dispersion: Rheology, preparation and characterization. *Polymer* **2017**, *123*, 55–64. [[CrossRef](#)]
37. Sultan, S.; Siqueira, G.; Zimmermann, T.; Mathew, A.P. 3D printing of nano-cellulosic biomaterials for medical applications. *Curr. Opin. Biomed. Eng.* **2017**, *2*, 29–34. [[CrossRef](#)]

38. Jessop, Z.M.; Al-Sabah, A.; Gao, N.; Kyle, S.; Thomas, B.; Badiei, N.; Hawkins, K.; Whitaker, I.S. Printability of pulp derived crystal, fibril and blend nanocellulose-alginate bioinks for extrusion 3D bioprinting. *Biofabrication* **2019**, *11*, 045006. [[CrossRef](#)]
39. Al-Sabah, A.; Burnell, S.; Simoes, I.N.; Jessop, Z.; Badiei, N.; Blain, E.; Whitaker, I.S. Structural and mechanical characterization of crosslinked and sterilised nanocellulose-based hydrogels for cartilage tissue engineering. *Carbohydr. Polym.* **2019**, *212*, 242–251. [[CrossRef](#)]
40. Maitra, J.; Shukla, V.K. Cross-linking in hydrogels—A review. *Am. J. Polym. Sci.* **2014**, *4*, 25–31.
41. Tang, A.; Wang, Q.; Zhao, S.; Liu, W. Fabrication of nanocellulose/PEGDA hydrogel by 3D printing. *Rapid Prototyp. J.* **2018**, *24*, 1265–1271. [[CrossRef](#)]
42. Mahanani, E.S.; Herningtyas, E.H.; Bachtiar, I.; Ana, I.D. Degradation profile and fibroblast proliferation on synthetic coral scaffold for bone regeneration. In *AIP Conference Proceedings*; AIP Publishing LLC: New York, NY, USA, 2016; Volume 1755, p. 160007. [[CrossRef](#)]
43. Siqueira, P.; Siqueira, É.; De Lima, A.E.; Siqueira, G.; Pinzón-García, A.D.; Lopes, A.P.; Segura, M.E.; Isaac, A.; Pereira, F.V.; Botaro, V.R. Three-dimensional stable alginate-nanocellulose gels for biomedical applications: Towards tunable mechanical properties and cell growing. *Nanomaterials* **2019**, *9*, 78. [[CrossRef](#)]
44. Bociaga, D.; Bartniak, M.; Grabarczyk, J.; Przybyszewska, K. Sodium Alginate/Gelatine Hydrogels for Direct Bioprinting—The Effect of Composition Selection and Applied Solvents on the Bioink Properties. *Materials* **2019**, *12*, 2669. [[CrossRef](#)] [[PubMed](#)]
45. Liu, T.; Lu, S.; Peng, X.; Jiao, C.; Zhang, J.; Han, M.; Wang, H. Tough, Stimuli-Responsive, and Biocompatible Hydrogels with Very High Water Content. *Macromol. Rapid Commun.* **2018**, *39*, e1800474. [[CrossRef](#)]
46. Armstrong, C.G.; Mow, V.C. Variations in the intrinsic mechanical properties of human articular cartilage with age, degeneration, and water content. *J. Bone Jt. Surg. Am.* **1982**, *64*, 88–94. [[CrossRef](#)]
47. Wan, L.Q.; Jiang, J.; Arnold, D.E.; Guo, X.E.; Lu, H.H.; Mow, V.C. Calcium Concentration Effects on the Mechanical and Biochemical Properties of Chondrocyte-Alginate Constructs. *Cell. Mol. Bioeng.* **2008**, *1*, 93–102. [[CrossRef](#)]
48. Cidonio, G.; Cooke, M.; Glinka, M.; Dawson, J.; Grover, L.; Oreffo, R. Printing bone in a gel: Using nanocomposite bioink to print functionalised bone scaffolds. *Mater. Today Bio* **2019**, *4*, 100028. [[CrossRef](#)] [[PubMed](#)]
49. Hussain, I.; Sayed, S.M.; Liu, S.; Oderinde, O.K.; Kang, M.; Yao, F.; Fu, G. Enhancing the mechanical properties and self-healing efficiency of hydroxyethyl cellulose-based conductive hydrogels via supramolecular interactions. *Eur. Polym. J.* **2018**, *105*, 85–94. [[CrossRef](#)]
50. Hatano, K.; Inoue, H.; Kojo, T.; Matsunaga, T.; Tsujisawa, T.; Uchiyama, C.; Uchida, Y. Effect of surface roughness on proliferation and alkaline phosphatase expression of rat calvarial cells cultured on polystyrene. *Bone* **1999**, *25*, 439–445. [[CrossRef](#)]
51. Bružauskaitė, I.; Bironaitė, D.; Bagdonas, E.; Bernotienė, E. Scaffolds and cells for tissue regeneration: Different scaffold pore sizes—Different cell effects. *Cytotechnology* **2016**, *68*, 355–369. [[CrossRef](#)]
52. Zhang, X.; Yu, Y.; Jiang, Z.; Wang, H. The effect of freezing speed and hydrogel concentration on the microstructure and compressive performance of bamboo-based cellulose aerogel. *J. Wood Sci.* **2015**, *61*, 595–601. [[CrossRef](#)]
53. Koch, M.; Włodarczyk-Biegun, M.K. Faithful scanning electron microscopic (SEM) visualization of 3D printed alginate-based scaffolds. *Bioprinting* **2020**, *20*, e00098. [[CrossRef](#)]